

**“The origin of the low-velocity anomalies beneath the rootless Atlas Mountains: insights gained from modeling of anisotropy developed by the travel of Canary Plume”**

Hwaju Lee<sup>1,2\*</sup>, Maximilano J. Bezada<sup>1</sup>, YoungHee Kim<sup>2</sup>

<sup>1</sup>School of Earth & Environmental Sciences, University of Minnesota, Minneapolis, Minnesota, USA

<sup>2</sup>School of Earth and Environmental Sciences, Seoul National University, Seoul, Republic of Korea

**Contents of this file**

Figure S1. The distribution of teleseismic events used in this study

Figure S2. The depth slice of the spatial distribution of the low-velocity anomalies that are slower than 2% P-wave velocity perturbation ( $dV_p/V_p$ ) below the Moroccan Atlas and northeast (NE) Morocco. The gray triangles present the stations.

Figure S3. Zoom-in views of anisotropy model EDC (top) and TwoStems (bottom) as examples.

Figure S4. SWS misfit between observed and predicted SWS using Matlab Seismic Anisotropy Tools (MSAT).

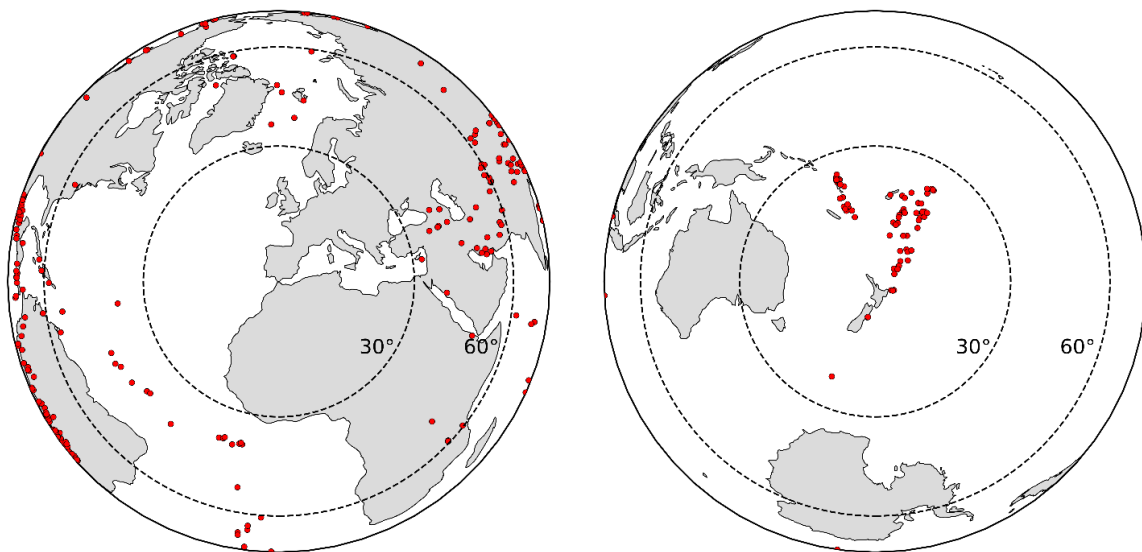
Figure S5. The depth slices show  $dV_p/V_p$  for one isotropy model and five anisotropy models.

Figure S6. Figure 3 in a 5%  $dV_p/V_p$  scale.

Figure S7. Lateral variation of  $dV_p/V_p$  for different models along the dashed-black line in Figure 3a.

## Introduction

This document includes Figure S1 to show the locations of the teleseismic events used in the study. Figures S2 and S3 are to support Figure 2. Figure S2 shows the spatial distribution of anisotropy models which is the same as the contour of  $-2\% \text{ dVp/Vp}$ . Figure 3 shows the zoom-in view of the anisotropy models. Figure S4 shows the SWS misfit between the observed and predicted SWS based on MSAT. Figure S5 shows the depth slices (60, 75, 90, 125, 160, 195, 270, 350, 480 km) of the tomographic result in addition to Figure 3. Figure S6 shows the cross-sectional views as well as depth slices at 125 km of the tomographic images on a  $5\% \text{ dVp/Vp}$  scale. Figure S7 quantitatively shows the change of the Vp along different depth slices.



**Figure S1.** The distribution of teleseismic events that were used in this study.

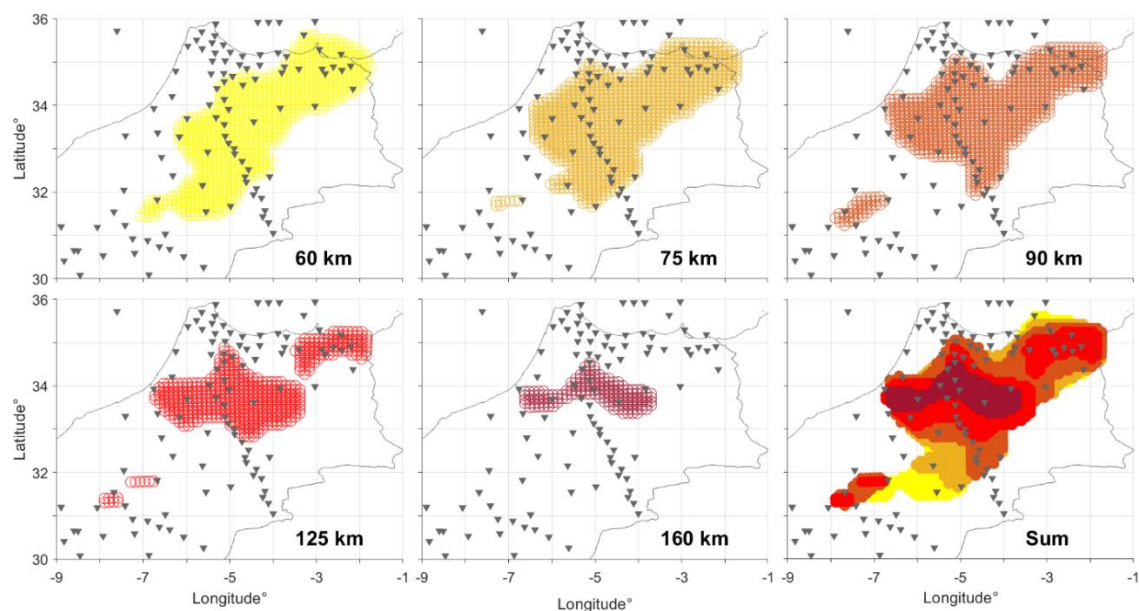


**Figure S2.** The depth slice of the spatial distribution of the low-velocity anomalies that are slower than 2% P-wave velocity perturbation ( $dV_p/V_p$ ) below the Moroccan Atlas and northeast (NE) Morocco. The gray triangles present the stations.

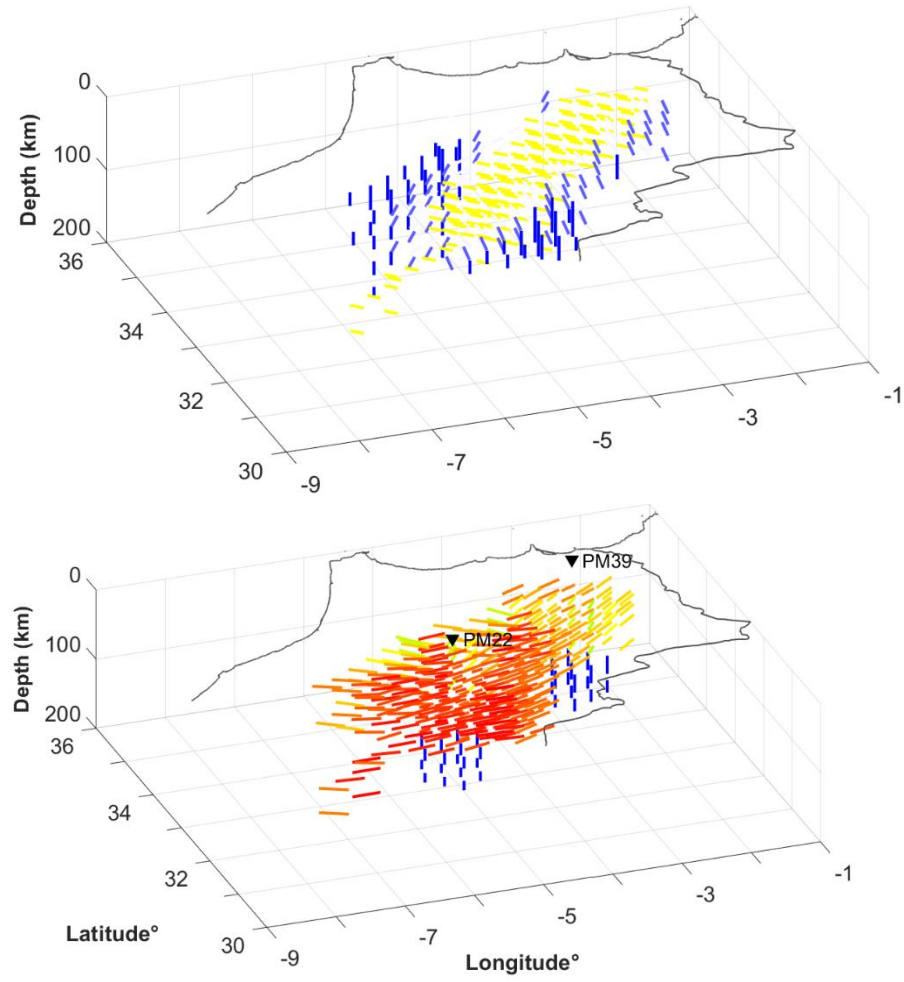


**Figure S3.** Zoom-in views of anisotropy model EDC (top) and TwoStems (bottom) as examples.

To predict the SWS produced by the anisotropy models, we utilize the Matlab Seismic Anisotropy Toolbox (MSAT) (Walker & Wookey, 2012) (see details in Lee et al. (2021)). To consider the misfits of FPD and time of SWS together, we measure the vector difference between observed and predicted SWS at each station. We use the mean of the vector difference at each station as the overall SWS misfit. As null splitting is expected when SFD is aligned parallel to the ray path (i.e., vertically aligned SFD to the surface), we find no splitting from the Isotropy and UpW as well as the upwelling portion of EDC. The MSAT misfits for both Isotropy and UpW are 1.098 seconds while EDC has the largest misfit of 1.103 seconds. We find the best misfit from Lateral, 0.678 seconds followed by OneStem (0.691 s) and TwoStems (0.721 s). As the stem portions of OneStem and TwoStems have the SFD aligned vertically (darker gray circles in Figure 4), the splitting above the stem regions is smaller than for model Lateral and this leads the misfit to be larger than in the same locations for model Lateral.

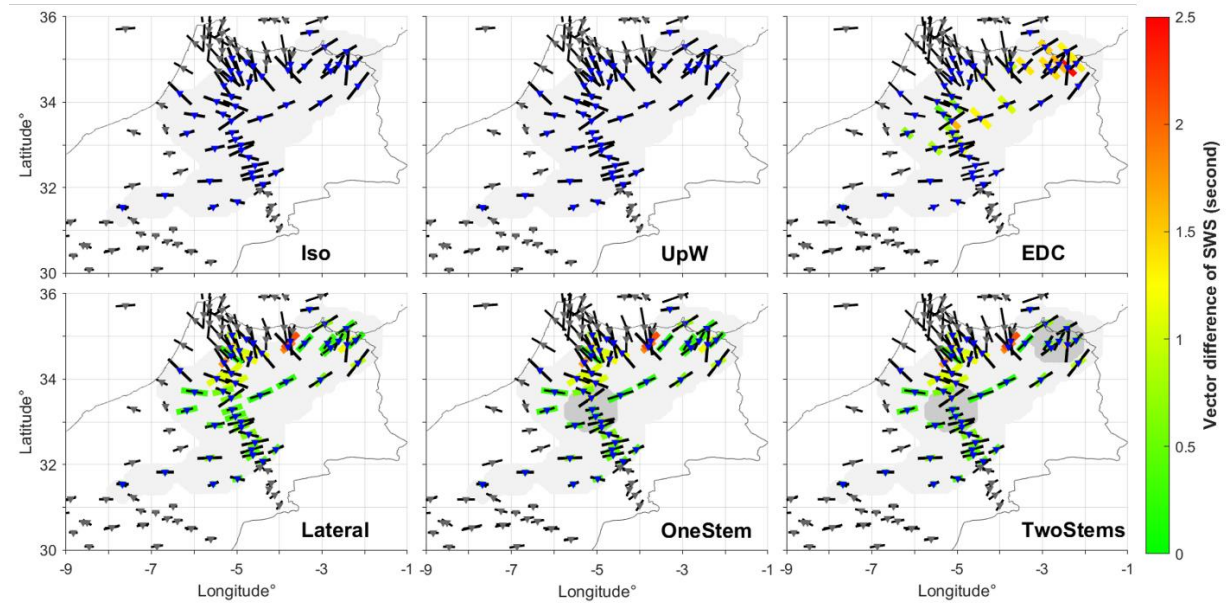


**Figure S4.** SWS misfit between the observed and predicted SWS. Matlab Seismic Anisotropy Tool (MSAT) is used for the predicted SWS. The light-gray shaded area represents the spatial distribution of anisotropy models while the darker-gray circles in OneStem and TwoStems represent the locations of the stems. The gray triangles present the location of the seismic stations of the study region while blue triangles present the stations where anisotropy models are placed among the grey stations. The black bars and colored bars present the observed SWS and predicted SWS based on MSAT, respectively. The predicted SWS are colored by vector difference between the observed and predicted SWS. As no splitting is expected from isotropy, there is no predicted SWS for the Iso (i.e., no anisotropy model). Also, no splitting is expected when SFDs of anisotropy are vertically aligned to the surface; consequently, MSAT does not exhibit any SWS for the model UpW.



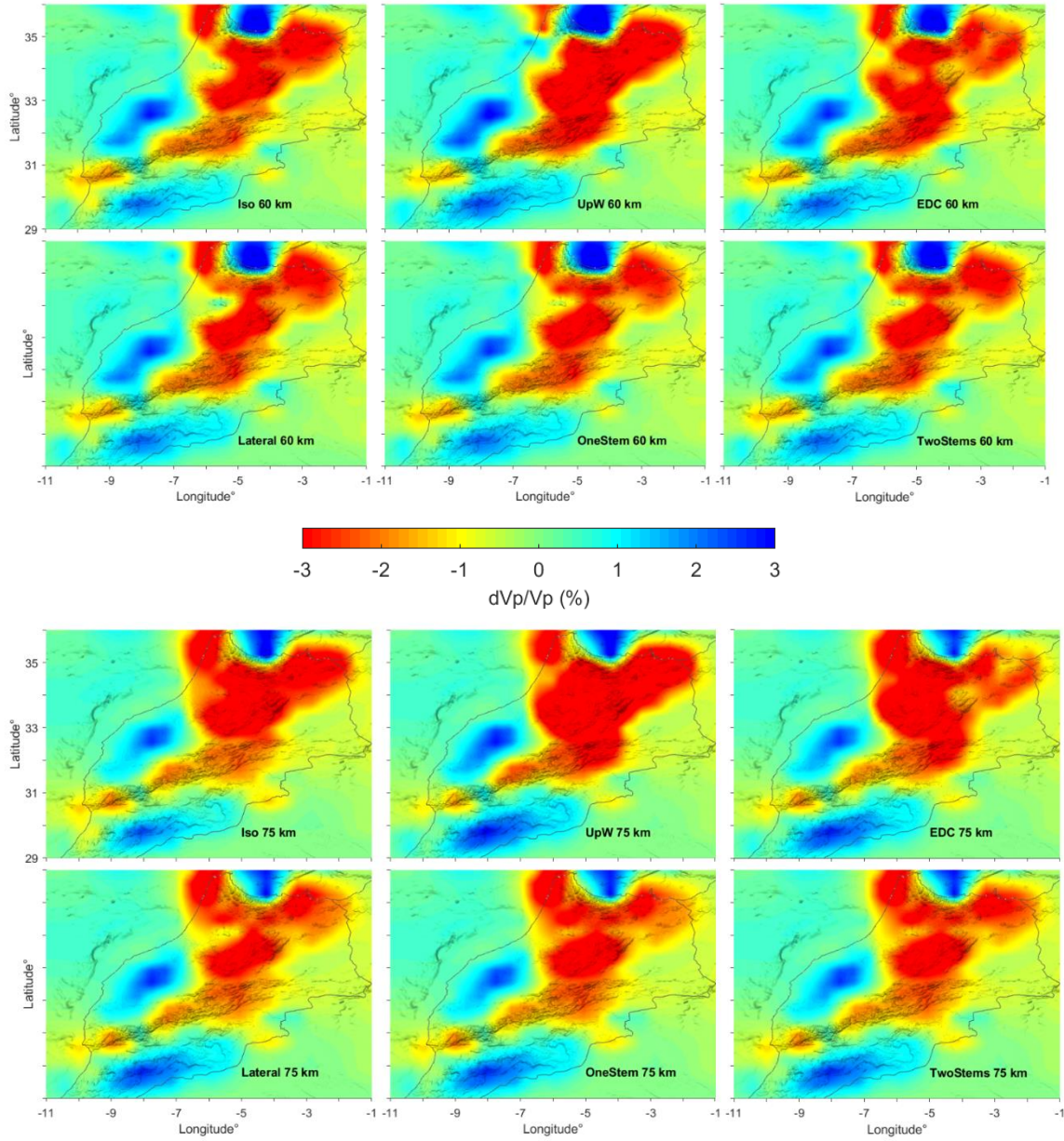


**Figure S5.** The depth slices (60, 75, 90, 125, 160, 195, 270, 350, 480 km) show  $dV_p/V_p$  for one isotropy model and five anisotropy models.

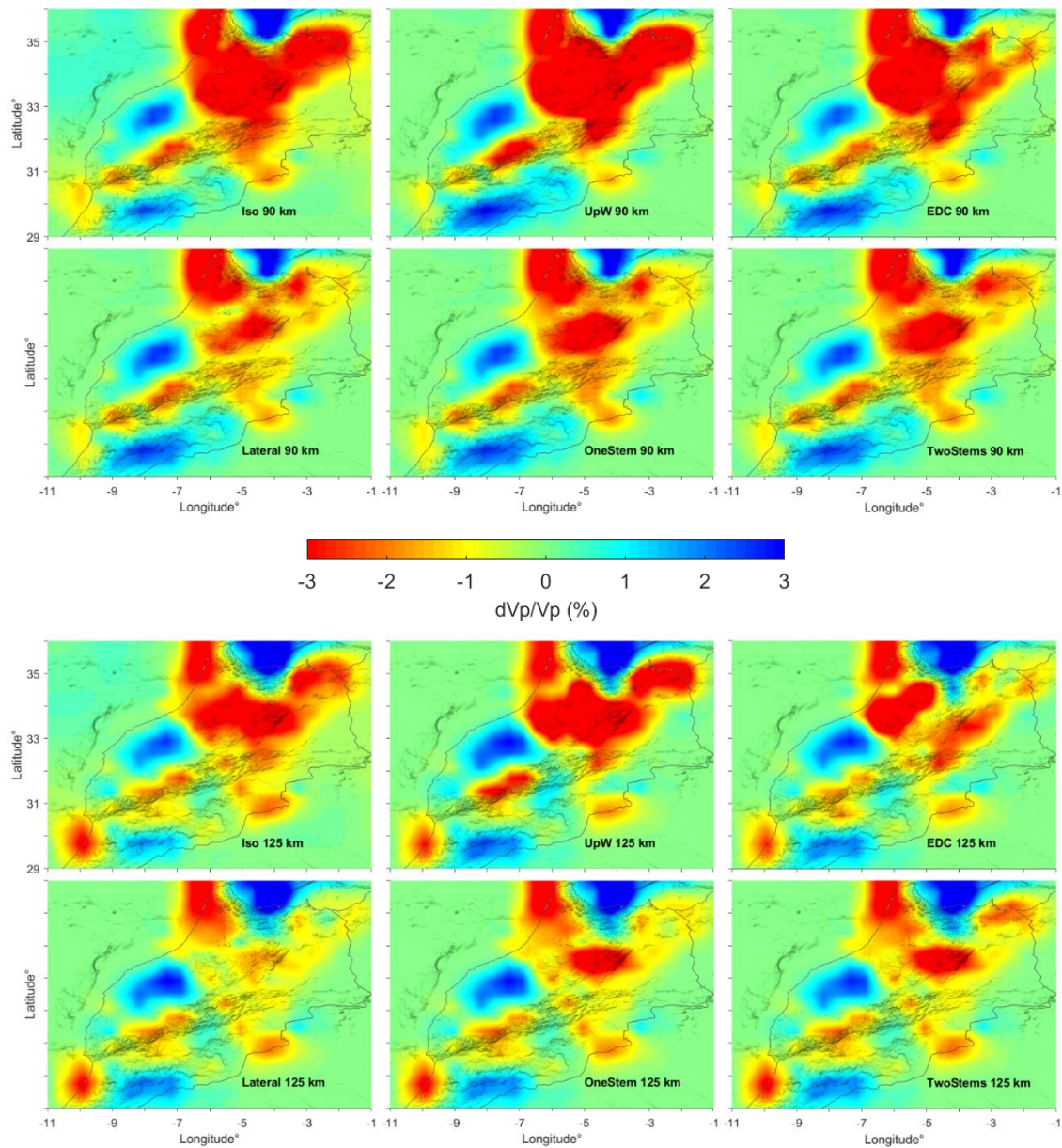


**Figure S5** (continued).



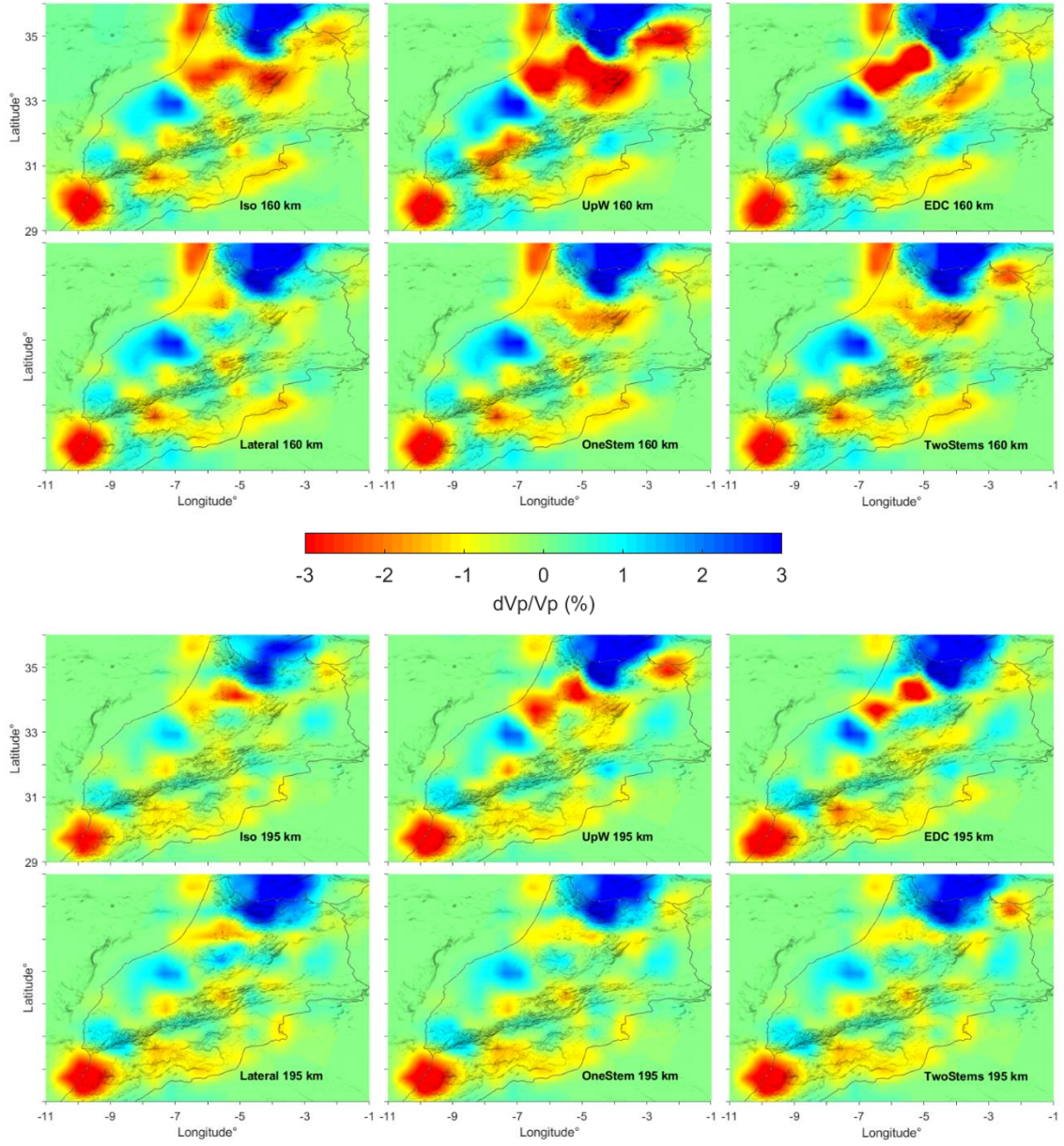


**Figure S5** (continued).



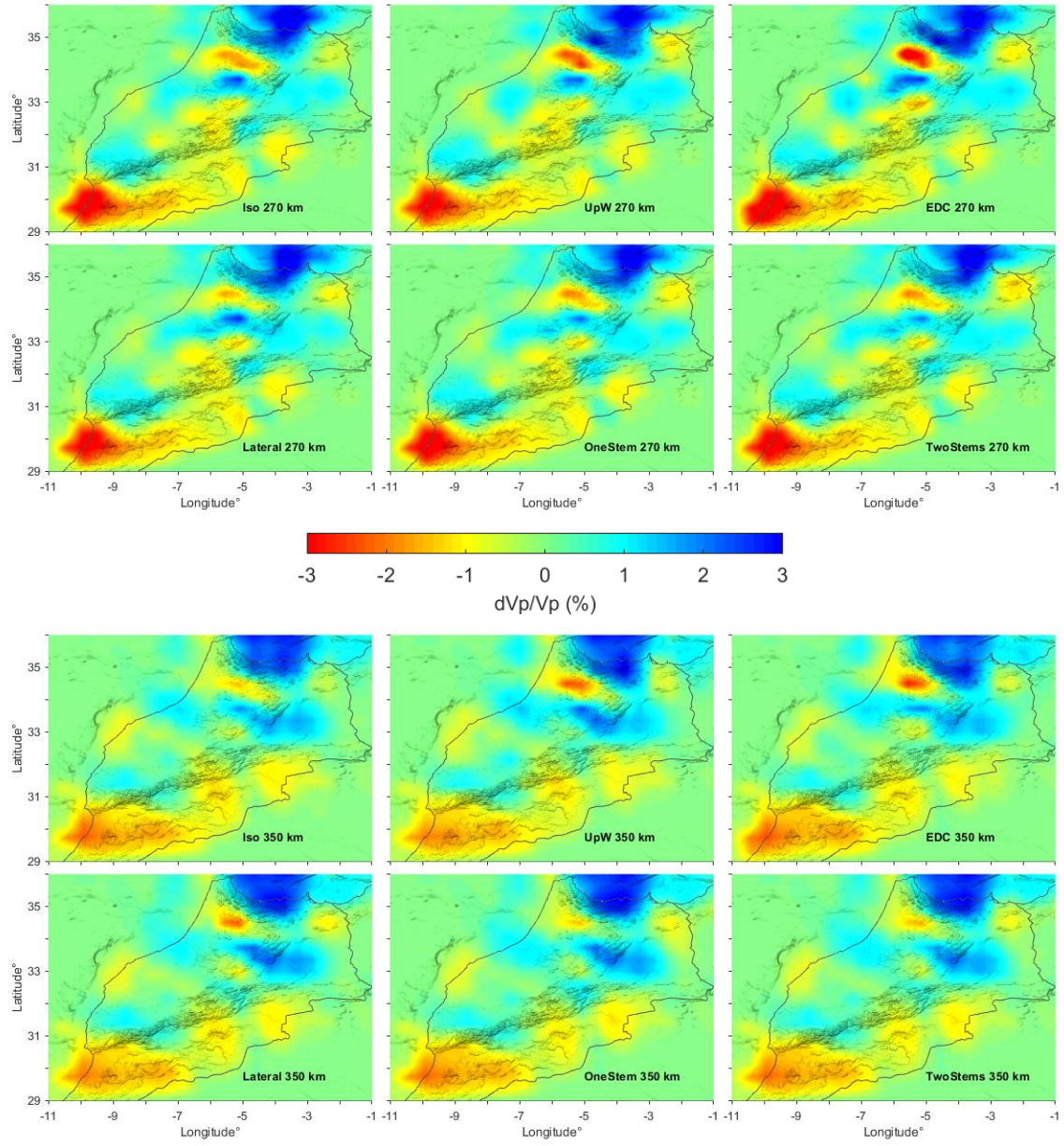


**Figure S5** (continued).

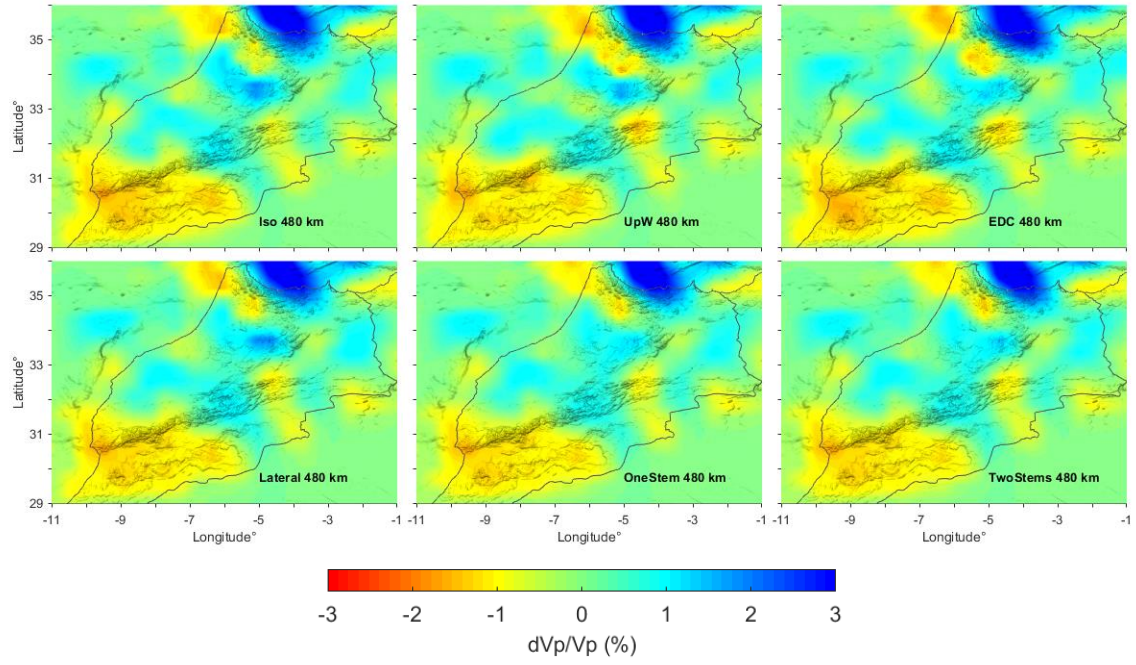


**Figure S5** (continued).



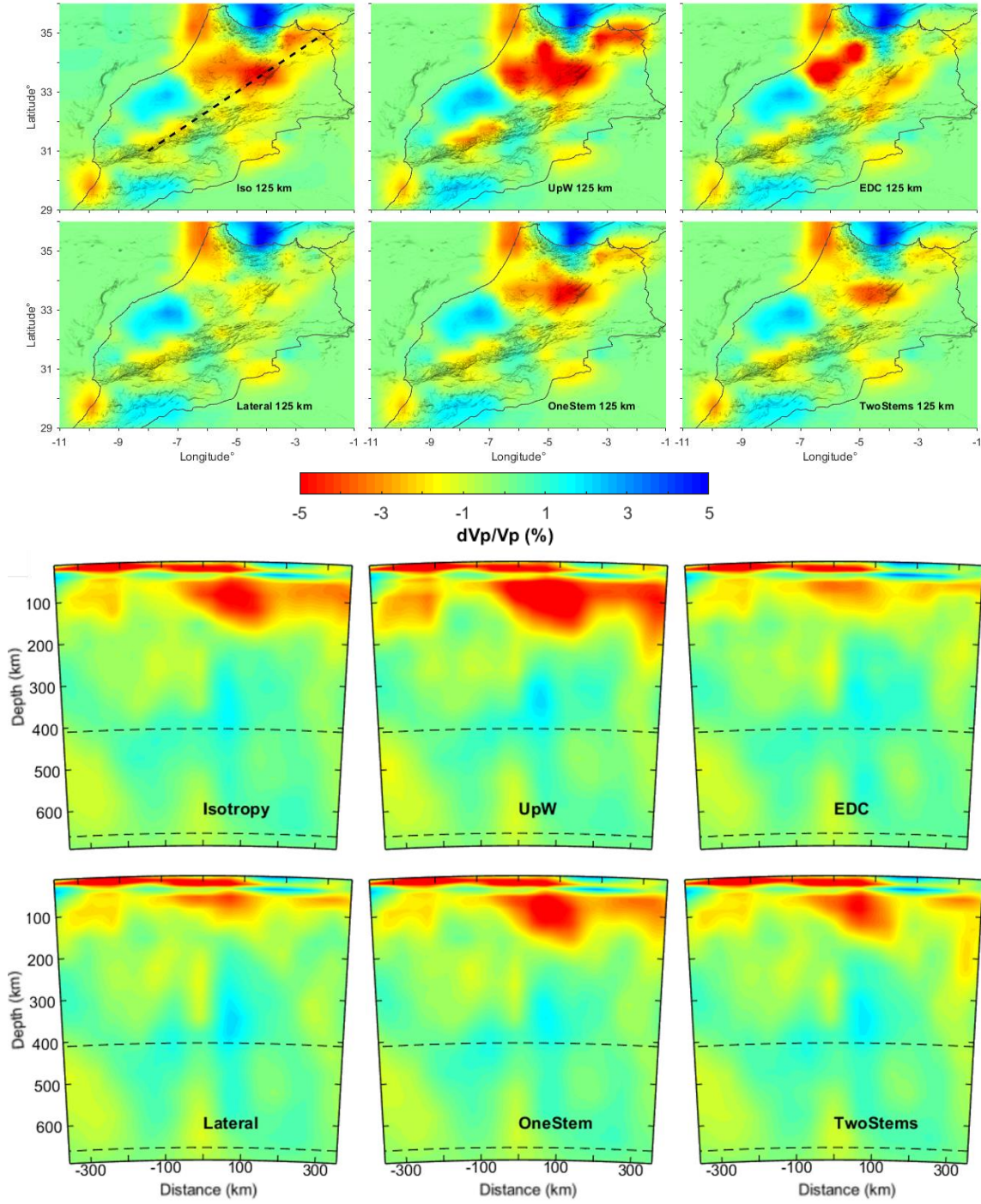


**Figure S6.** The top six panels are tomographic slices at 125 km depth of the isotropy and anisotropy models. The bottom six panels show the cross-sectional view of the tomographic result along with the line between [31°N, 8°W] and [35°N, 2°W]. The tomographic images are in a  $\pm 5\%$   $dVp/Vp$  scale instead of a  $\pm 3\%$   $dVp/Vp$ .

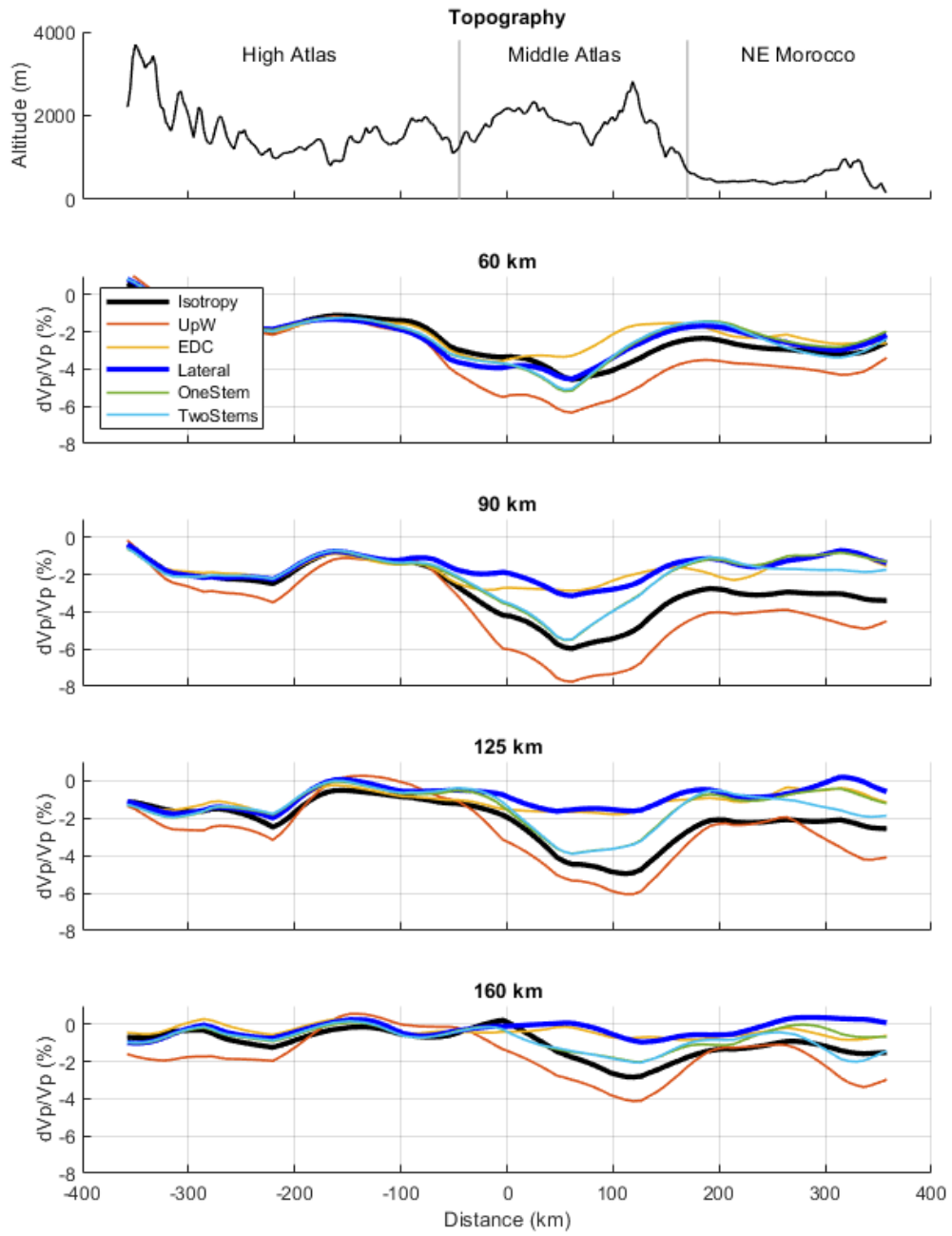


**Figure S7.** Lateral variation of  $dV_p/V_p$  for different models along the dashed-black line in Figure 3a.